

# Modeling and Measurement of Glass Transition Temperatures of Energetic and Inert Systems

Mounir Jaidann,<sup>1,2</sup> Hakima Abou-Rachid,<sup>1</sup> Xavier Lafleur-Lambert,<sup>1,2</sup> Louis-Simon Lussier,<sup>1</sup> Nicole Gagnon,<sup>1</sup> Josée Brisson<sup>2</sup>

<sup>1</sup> Defence Research and Development Canada, Québec, Canada G1X 3J5

<sup>2</sup> Centre de Recherche en Science et Ingénierie des Macromolécules (CERSIM), Département de Chimie, Faculté des Sciences et de Génie, Université Laval, Québec, Canada G1K 7P4

In this article, measurements of glass transition temperature ( $T_g$ ) changes of two energetic material blend systems were carried out using the differential scanning calorimetry (DSC) technique. On one hand, experimental  $T_g$  values were compared to those predicted by the additivity model, Fox and Pochan equations, and, on other hand, to atomistic molecular dynamics simulation results performed in this work. The two blend systems studied were both composed of a polymer, either the inert hydroxyl-terminated polybutadiene (HTPB) or the energetic polyglycidylazide (GAP), and smaller molecules, which acted as plasticizers, dioctyl adipate (DOA), or glycidylazide oligomers (Gp1). Modeling results show deviations from experimental data, which varied from 5 to 20 K over an absolute scale for pure components and blends. A good fit was found when predicting the effect of adding smaller molecules to HTPB. Simulations were particularly useful for the blend in which the glass transition temperature of one component, DOA, was not experimentally measurable, due to the high crystallinity of the small DOA molecule. POLYM. ENG. SCI., 48:1141–1150, 2008. © 2008 Society of Plastics Engineers

## INTRODUCTION

The next generations of plastic-bonded explosives (PBX) materials will possess improved insensitivity and energetic density while maintaining a good mechanical integrity. Atomistic molecular modeling may become a helpful tool in the conception of these formulations, providing predictions on various properties of these systems. This may decrease hazards and accidents during the development of these formulations as well the time-frame in which they can be screened and tested, eliminating poor formulations before even having to synthesize the compounds.

To be insensitive, the explosive must have a way to disperse the energy given upon a shock. Most explosives exist as elastomeric preparations, in which such energy can be dispersed easily as long-range movements, which occur and are typical of the elastomeric or rubber state. However, at the glass transition temperature, abbreviated  $T_g$ , materials changes from this rubber state to the glassy state, in which such long-range movements do not exist. At this temperature, explosives therefore loose their elastomeric properties and the possibility of energy dissipation through long-range movements. Resulting degradation of mechanical properties is such that Stacer and Husband have proposed glass transition temperature as a failure criterion for explosive formulation [1]. Evaluating the predictive methods for energetic molecules and materials with respect to  $T_g$  is therefore of strategic interest.

Despite its importance for polymer properties, the nature of the glass transition is still the object of considerable controversy. Many models have been proposed to explain this transition, the most widely used including the thermodynamic model [2], the kinetic model [3], and the free volume model, which incorporates kinetic and thermodynamic aspects [4]. In general, glass transition is attributed to a second-order thermodynamic transition, and a discontinuity with temperature is expected for all state properties. It is however clearly established that the glass transition temperature also incorporates a clear kinetic effect [5].

Many empirical or theoretical approaches have been proposed to predict  $T_g$  values for blends. By far, the simplest is the additivity law [6],

$$T_g = w_1 T_{g1} + w_2 T_{g2} \quad (1)$$

where  $w_i$  ( $i = 1, 2$ ) represents the weight or the volume fraction of a pure component  $i$ , and  $T_{gi}$  its individual glass transition temperature. Other completely independent

Correspondence to: Hakima Abou-Rachid or Josée Brisson; e-mail: hakima.abou-rachid@drdc-rddc.gc.ca or josee.brisson@chm.ulaval.ca

Contract grant sponsor: Defence Research and Development Canada.

DOI 10.1002/pen.21062

Published online in Wiley InterScience (www.interscience.wiley.com).

© 2008 Society of Plastics Engineers

equations have been proposed, the most used being the empirical equation proposed by Fox in 1956 [7],

$$\frac{1}{T_g} = \frac{w_1}{T_{g1}} + \frac{w_2}{T_{g2}} \quad (2)$$

which does not require any additional parameter. Later, in 1979, Pochan et al. [8] also proposed an empirical Eq. 5 and used Fox equation for purposes of comparison for a great number of mixed amorphous systems,

$$\ln T_g = w_1 \ln T_{g1} + w_2 \ln T_{g2} \quad (3)$$

Equation 3 is often referred to as the Pochan equation and could be extended to multicomponents solutions. The advantage of Fox and Pochan descriptions of the  $T_g$  for mixed systems is that are based only on the knowledge of the individual  $T_{gi}$  of the pure components and on blend composition (weight or volume fractions). More general equations based on thermodynamic considerations, including refinements, have been proposed by Gordon-Taylor [9], Kovacs [10], or Schneider [11]. These equations allow a better matching with experimental data. However, they require too many additional parameters to be used as predictive tools. For systems with strong interactions, major deviations to these equations were observed, and, in 1984, Kwei [12] proposed an empirical correction to the Gordon-Taylor equation, in which an adjustable parameter named  $q$  is added to take into account intermolecular forces between blend components. This provides a better matching with experimental data, but this equation cannot be used for predictive purposes. Therefore, additivity, Fox and Pochan equations are the three main predictive approaches that can be used when experimental data on pure components is limited. To conclude, Simha [13] pointed out in his work that no quantitative theory exist based on first principles showing the existence as well as the location of the glass transition temperature  $T_g$ . In addition, Somcynsky and Simha [14] stated in their work that any model that describes the glass transition temperature using only one single parameter remains questionable, because it cannot predict correctly the observed behavior in various conditions of volume, pressure, and temperature properties at the glass temperature.

Rigby and Roe [4] have proposed the use of molecular dynamics (abbreviated MD) to gain information on glass transition. They showed that polyethylene models built by molecular modeling presented discontinuities versus temperature of specific volume, diffusion coefficient [15], and free volume [4], which they associated to the glass transition temperature phenomena. Such discontinuities also occur for other polymer simulations [16–18] and a literature review on  $T_g$  simulation by molecular dynamics was published by Boyd [19]. The use of MD for glass transition simulations has been seriously criticized, because the cooling speed used in modeling simulations are orders of magnitude faster than the expected relaxation time of an

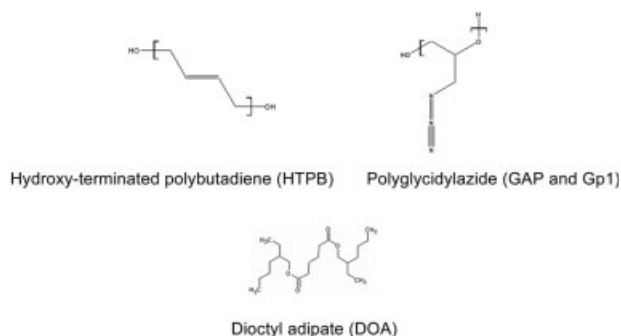


FIG. 1. Chemical structures of studied molecules.

entangled melt, which is of the order of  $10^{-6}$  s. It was concluded that the molecular modeling cannot be used to reach the equilibrium state and therefore that calculated properties could represent correctly those at equilibrium [20]. Nevertheless, it is more and more accepted that movements responsible for or associated to the increase in free volume at  $T_g$  are reproduced with sufficient accuracy by molecular modeling simulations, and that this technique provides reliable estimates of the glass transition temperature. There is general agreement on the fact that a variable shift in glass temperature is observed when comparing modeling values to experimental value. Molecular modeling has also been used to simulate the  $T_g$  of polymer blends [21], and, more recently, the effect of a plasticizer on a polymer [22].

In this work, experimental DSC data on energetic formulations are reported and used to evaluate the usefulness and reliability of energetic material  $T_g$  temperatures obtained by molecular modeling, by classical additivity law or by the Pochan and Fox approaches. Two 50:50 blend formulations comprising energetic molecules were selected: a hydroxyl-terminated polybutadiene (HTPB) and dioctyl adipate (DOA) blend, in which the two blended molecules present important structural differences, as can be seen in Fig. 1, and a blend comprising two molecules having the same chemical structure but different molecular weights, polyglycidylazide (GAP), where GAP is a high molecular weight material plasticized by its oligomer, Gp1.

## Methodology

**Experimental.** The hydroxyl-terminated polybutadiene (Poly Bd<sup>®</sup> R-45M resin) was provided by Sartomer [23], with a molecular weight  $M_w$  of  $2,800 \text{ g mol}^{-1}$ . The GAP polymer and GAP plasticizer were provided by 3 M Corp ( $M_w$  of 5000 and  $700 \text{ g mol}^{-1}$ , respectively), and the dioctyl adipate came from Canada Colors and Chemicals.

Experimental glass transition temperatures were measured by a model Q2000 differential scanning calorimeter (DSC) from TA Instruments. Each standard DSC cell contained 4–8 mg of pure polymer or a 50 w% mixture of polymer/plasticizer solution prepared at room temperature.

TABLE 1. Amorphous unit cell composition.

Systems	$N_{\text{poly}}$	$N_{\text{plas}}$	$N_{\text{mon}}$	$N_{\text{at}}$	$X_{\text{w}}$	$X_{\text{m}}$	$\rho_{\text{exp}}$	$\rho_{\text{i}}$	$\rho_{\text{f}}$	$a$
HTPB (Model 1)	2	0	53	1028	0.000	0.000	0.899	0.900	0.893	21.83
HTPB (Model 2)	1	0	371	3574	0.000	0.000	0.899	0.900	0.866	33.35
HTPB/DOA	1	8	53/1	1058	0.514	0.875	—	0.915	0.916	21.92
GAP	1	0	50	603	0.000	0.000	1.300	1.300	1.277	18.62
GAP/GpI	1	7	50/7	1205	0.495	0.857	—	1.270	1.288	23.40
GpI	0	12	7	1032	1.000	1.000	1.240	1.240	1.261	22.32

$N_{\text{poly}}$ ,  $N_{\text{plas}}$ , and  $N_{\text{mon}}$  are the number of polymer molecules, plasticizer molecules, and monomers per polymer chain, respectively.  $N_{\text{at}}$  is the total number of atoms unit cell.  $X_{\text{w}}$  and  $X_{\text{m}}$  are the plasticizer weight and mole fraction, respectively.  $\rho_{\text{exp}}$ ,  $\rho_{\text{i}}$ , and  $\rho_{\text{f}}$  are the experimental, initial, and final density, respectively, in  $\text{g/cm}^3$ , and at 300 K,  $a$  is the final unit cell dimension in Angstrom.

The melting point of indium was used to calibrate the apparatus. Each mixture was prepared by combining 2–4 mg of polymer with an equal plasticizer mass. The analyses were carried out with a heating rate of  $10^\circ\text{C/min}$ , starting from a temperature of  $-120^\circ\text{C}$ , and raising the temperature of the sample up to  $150^\circ\text{C}$ . Glass transition temperature is reported as the transition midpoint, as determined from three tangent lines, in all cases.

**Model Construction and Validation.** MD was performed using the Discover and Amorphous Cell software modules of the Materials Studio package, Accelrys, installed on a SGI Altix 3000 high-end server, using a maximum of four processors due to license limitations. COMPASS, an ab initio force field optimized for the condensed phase, was chosen. It has been previously used to predict PVT properties various polymers [24–27] and energetic molecules [28]. The NPT ensemble (constant number of particles, pressure and temperature) was used for the MD glass transition temperature simulations, with the pressure fixed at zero bar, an approximation deemed acceptable by Han et al. [16] who validated this approach for many different types of polymers. The pressure and temperature in all the dynamics simulations were controlled respectively by the Berendsen (decay constant of 0.1 ps) and Andersen (collision ratio of 1.0) algorithms. In all cases, the Verlet velocity algorithm was used for integration, with an integration step of 1 ps and a cut-off distance for nonbond interactions of 9.5 Å. Under periodic boundary conditions, van der Waals interactions were calculated using a cut-off distance of 9.5 Å, using a spline width of 1 Å and a buffer width of 0.5 Å. Ewald summation was used for evaluation of long-range coulombic interactions, with an Ewald accuracy of  $10^{-2}$  and an update width if 1.00.

For HTPB Model one, a 53 repeat unit chain ( $M_{\text{w}} = 2,790 \text{ g mol}^{-1}$ ) was generated unit by unit, using a random copolymer propagation algorithm with probabilities for the configurations at 0.6 for trans-1,4, 0.2 for cis-1,4 and 0.2 for vinyl-1,2. The HTPB Model two was constructed in a similar fashion, using a larger 371 repeat unit chain ( $M_{\text{w}} = 19,530 \text{ g mol}^{-1}$ ). A 50 repeat unit GAP chain ( $M_{\text{w}} = 4,970 \text{ g mol}^{-1}$ ) and a seven repeat unit GpI

plasticizer chain ( $M_{\text{w}} = 700 \text{ g mol}^{-1}$ ) were constructed. HTPB and Gap were given hydroxyl end groups, as is the case in the polymers studied experimentally. GpI was given hydrogen end groups. All initial molecules were then subjected to energy minimization using successively steepest descent, conjugate gradient, and Newton techniques, until derivatives were less than  $0.00001 \text{ kcal mol}^{-1}$ .

Both polybutadiene amorphous models were created using the approach developed by Theodorou and Suter, as implemented in the Amorphous Phase module of Materials Studio. One substrate with a width of 20 K was used at each step to ensure a more uniform filling of the available space. These models were constructed at the experimental density of  $0.90 \text{ g cm}^{-3}$  under periodic boundary conditions. However, in Model one, two 53 repeat unit chains were used, whereas Model two was built using a single, 371 repeat unit chains. Other systems were built in a similar fashion, although number of atoms and density of each system was different. Details on amorphous cell models are given in Table 1. In all cases, at least three models were created for each system.

Each system was relaxed using an NPT ensemble at 298 K until internal and external energy as well as density was found to fluctuate around a constant mean value, which took 100–200 ps. Room temperature density was estimated as an average over an additional 50 ps dynamics simulation. At this stage, the model, which yielded the lowest energy of each system, was selected for  $T_{\text{g}}$  determination.

A second equilibration was performed at a temperature 100 K above the expected glass transition temperature for an additional 300 ps. Density was measure as the average over the last 50 ps of this simulation. Temperature was decreased by 10 K steps, and each time re-equilibration was performed during 150 ps, density being measured for the next 50 ps of the simulations. Density values obtained at these various temperatures were used to draw a specific volume versus temperature curve in each case. Linear regression was first performed, using Microsoft Excel, on visually selected portions of the curves, starting with the lower temperature section. As, for data at temperatures near the breakpoint, data fluctuations were often

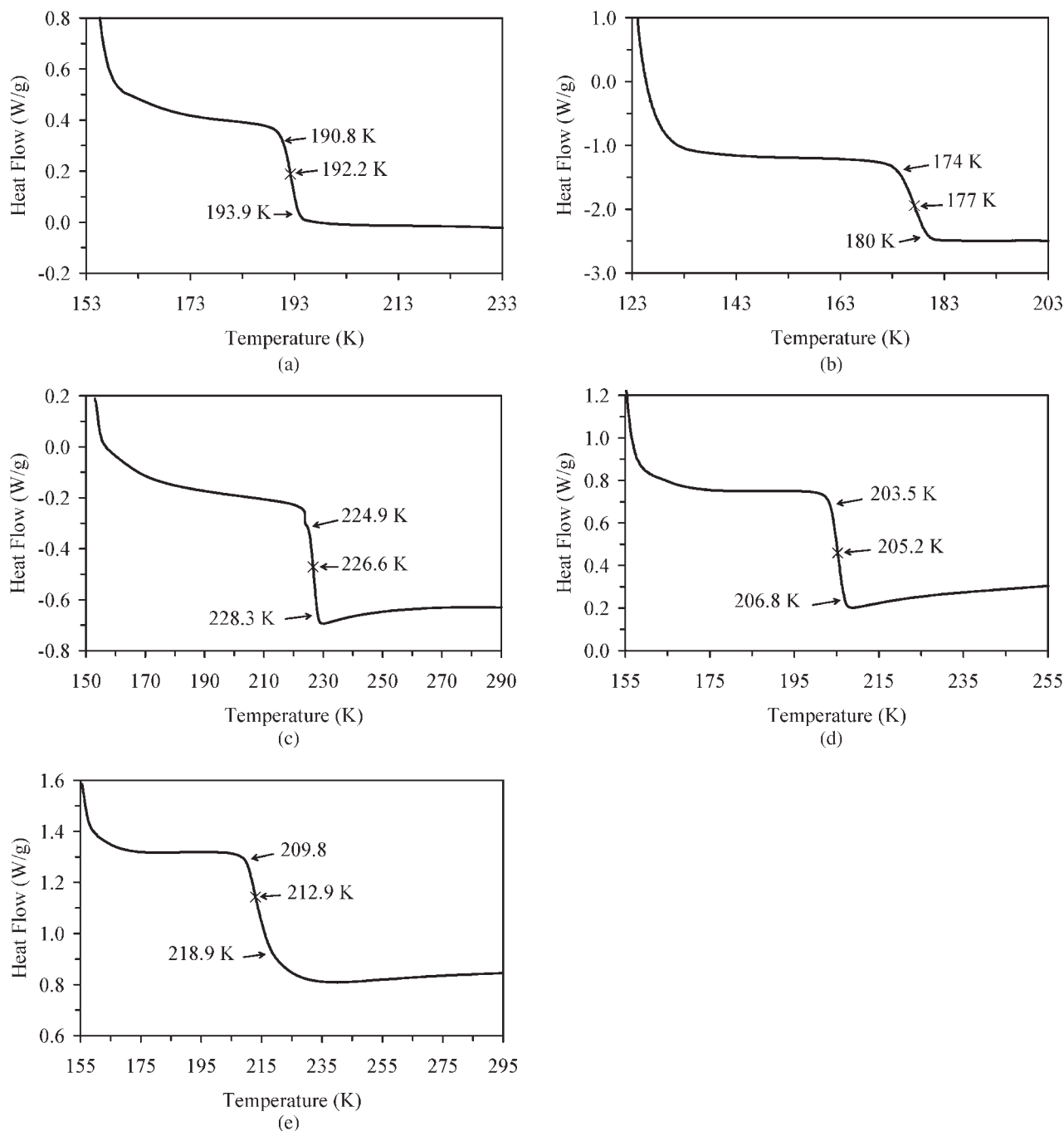


FIG. 2. Differential scanning calorimetry endotherms of pure components and blends, measured at a speed of  $10^{\circ}/\text{min}$ . (a) HTPB, (b) HTPB/DOA, (c) GAP, (d) Gp1, and (e) GAP/Gp1.

important, linear regression was performed on various alternate datasets, incorporating points near the breakpoint one by one to either the below- $T_g$  data set or the above- $T_g$  dataset. Each point was assigned to one of the sets on the basis of the best correlation coefficient. This procedure was performed until correlation coefficient was optimized for both datasets.

The glass transition temperature  $T_g$  was assessed as the intersection of the two linear regression straight lines. Confidence intervals were calculated using the Origin 6.1 Software at a 90% probability level and used to estimate

the error associated to  $T_g$  values predicted by this method.

## RESULTS AND DISCUSSION

### *Experimental Determination of the Effect of Plasticizer on Blends*

DSC was performed on studied blends. These will serve as a benchmark to estimate simulation validity. In all cases, these were taken under the same conditions, as

TABLE 2. Glass transition temperature values in kelvin provided by experiments ( $T_{g \text{ exp}}$ ), and calculations using different theoretical approaches ( $T_{g \text{ calc}}$ ) and molecular dynamics ( $T_{g \text{ MD}}$ ).

System	$T_{g \text{ exp}}^a \pm 5$	$T_{g \text{ calc}}$	$\Delta T_{g \text{ calc-exp}}$	$T_{g \text{ MD}}$	$\Delta T_{g \text{ MD-exp}}$	C1	C2
HTPB Model 1	192 <sup>a</sup> –198 <sup>b</sup>	—	—	201 $\pm$ 10 <sup>c</sup>	3–9	1.0000	0.9298
HTPB Model 2	192 <sup>a</sup> –198 <sup>b</sup>	—	—	200 $\pm$ 3 <sup>c</sup>	2–8	1.0000	0.9882
HTPB/DOA	177 <sup>a</sup>	—	—	183 $\pm$ 5 <sup>c</sup>	6	0.9946	0.9828
GAP	227 <sup>a</sup> –237 <sup>d</sup>	—	—	240 $\pm$ 5 <sup>c</sup>	3–13	0.9671	0.9665
GAP/Gp1	213 <sup>a</sup> –218 <sup>d</sup>	209 <sup>e</sup> –215 <sup>f</sup>	2–9	228 $\pm$ 10 <sup>c</sup>	10–15	0.9620	0.9351
Gp1	205 <sup>a</sup>	—	—	225 $\pm$ 8 <sup>c</sup>	20	0.9945	0.8842

<sup>a</sup> Experimental, this work.

<sup>b</sup> Ref. [24].

<sup>c</sup> MD, this work.

<sup>d</sup> Ref. [31].

<sup>e</sup> Additivity approach, this work.

<sup>f</sup> Fox and Pochan equations, this work.

$\Delta T_{g \text{ calc-exp}}$  and  $T_{g \text{ MD-exp}}$  express the difference between calculated (calc) or molecular dynamics (MD) values and experimental (exp) values. C1 and C2 are the correlation coefficient in MD for glassy phase and rubber phase, respectively.

it is well known that  $T_g$  values change with scanning speed due to kinetic effects. However, other factors also affect experimental values, such as molecular weight, structural and end-group defects, impurities, or humidity, which must be kept in mind when comparing to previously published experimental values.

Figure 2 reports typical DSC scans of pure components and blends. No DOA scan is reported, as this molecule is highly crystalline, and no glass transition could be detected. As can be seen from the figure, addition of DOA to HTPB results in a decrease in the temperature at which the heat capacity jump typical of glass transition is detected. Transition width, however, does not change with blending. These two observations are consistent with miscibility and the absence of phase separation at the scale to which DSC is sensitive, which has been reported to be around 10–50 nm [29, 30]. Similar observations are made on the GAP-Gp1 blend. Observed transition temperatures,  $T_{g \text{ exp}}$ , are reported in Table 2, along with literature values when available. Differences of 5–10 K are observed when comparing these values, which could be due to minor structural differences or scanning speed, as the latter is not reported.

Table 2 also reports calculated glass transition temperature values  $T_{g \text{ calc}}$  predicted using different models, which include the additivity approach, the Fox equation and the Pochan equation. Values can be compared only in one case, the GAP/Gp1 blend, for which a 6 K difference exists between  $\Delta T_{g \text{ calc}}$  values obtained when using the additivity approach and the Fox and Pochan equations. This is of the same order of magnitude as both the experimental precision of the technique and variations in experimental glass transition temperatures. Predictions are therefore quite acceptable, the Fox and Pochan equations resulting in better fits with experimental data, as expected.

Comparison can also be made on the basis of the decrease in  $T_g$  of the polymer upon plasticizer addition as experimental and predicted  $\Delta T_g$ , reported in Table 3. The

additivity approach yields the largest value of 18 K, Fox and Pochan equations are the smallest, with 12 K, whereas experimental data measured in this study yield an intermediate value of 14 K, and literature data yield the largest value with 19 K. All three approaches can therefore be used for predicting the glass transition temperature with similar success, although the Fox and Pochan equations fit better the experimental data presented here.

However, no prediction could be made on the HTPB system, due to the lack of experimental data on  $T_g$  of the amorphous phase of highly crystalline DOA. Unfortunately, this is not an exception, as most small molecules used as plasticizers are highly crystalline, and their  $T_g$  is usually unknown. Furthermore, to measure their glass transition temperatures, it is essential to synthesize or otherwise obtain them, which is not necessary with molecular modeling.

The two systems studied here both exhibited a modest experimental  $\Delta T_g$  value (15 for HTPB/DOA and 14 for GAP/Gp1). For the latter system, this can be attributed to a small  $T_g$  difference between pure components (only 22 K), and it can safely be assumed that this is also the case for the HTPB/DOA system. Under these conditions,

TABLE 3. Plasticizing effect comparison, as estimated by the decrease in  $T_g$  of the pure polymer  $\Delta T_g$  as estimated from experimental and predictive methods,  $\Delta T_g$ , in kelvin.

System	Experimental $\Delta T_g$	Predicted $\Delta T_g$
HTPB/DOA	15 <sup>a</sup>	18 <sup>b</sup>
GAP/Gp1	14 <sup>a</sup> , 19 <sup>c</sup>	12 <sup>b,d,e</sup> , 18 <sup>c</sup>

<sup>a</sup> Experimental, this work.

<sup>b</sup> MD, this work.

<sup>c</sup> Ref. [35].

<sup>d</sup> Fox and Pochan equations, this work.

<sup>e</sup> Additivity approach, this work.



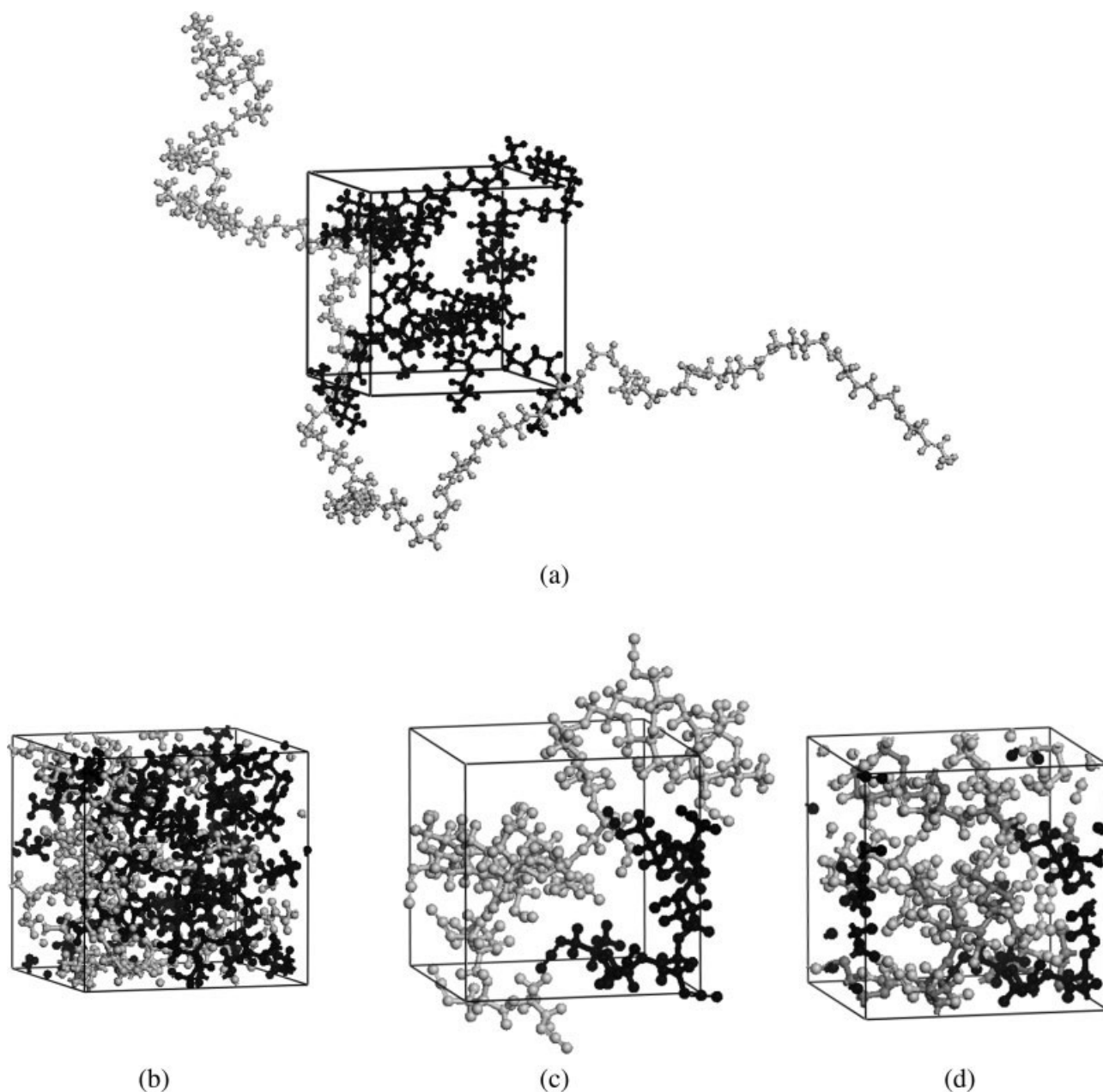


FIG. 3. Typical amorphous cell models for blends. Molecules (a) and (c) as placed with respect to unit cell for HTPB/DOA blend and GAP/Gp1 blend, respectively. Packed cell (b) and (d) content under periodic boundary conditions for HTPB/DOA blend and GAP/Gp1 blend, respectively.

any technique would basically give similar predicted values. Should a plasticizer-polymer system with a considerably different  $\Delta T_g$  be considered, prediction reliability would probably be much lower, and even more so if specific interactions, such as hydrogen bonds or ionic interactions, were present.

#### *Molecular Dynamics Simulations of Amorphous Phases*

Atomistic molecular mechanics can be used to create amorphous or crystalline phase models and can further be used to predict miscibility of energetic molecules [32]. In this work, Materials Studio was used to model amorphous

phases, using the Theodorou approach. A representative model of each blend is reported in Fig. 3 under two visualization modes. On the left, whole polymeric chains and plasticizer molecules are shown as placed within the unit cell, those created by periodic boundary conditions, or image molecules, being absent. The polymer is drawn in gray, and its continuity and random shape can clearly be seen. The plasticizer molecules, shown in black, adopt random positions with respect to the polymer chain. On the right, packed cells (under periodic boundary conditions), showing parent and image molecules, show the total cell contents. As can be seen, for both blends, compact models are obtained, the space fully is used, and no

specific organization can be visually detected, contrarily to a crystalline cell.

Initial models were equilibrated at room temperature and re-equilibrated at higher temperatures under NPT conditions. In each case, pair correlation function diagrams  $g(r)$  versus interatomic distance  $r$ , shown in Fig. 4, allows ascertaining the spatial distribution of atoms with respect to their neighbors. In both cases, absence of narrow peaks confirms the lack of periodicity, as expected in amorphous models. For both blends, the polymer–plasticizer curve is clearly at higher values than the polymer–polymer and plasticizer–plasticizer curves in the blends, indicative of a high degree of interactions between the two blend components. This feature is typical of miscible systems, in agreement with experimental observations. For the HTPB-DOA curve, the presence of a slight maximum around 6–8 Å may be associated with a correlation hole: at certain distances, intermolecular contacts are limited due to a screening effect of electronic cloud, which hinders atomic closeness. The observed maximum relates to the position of the first closest neighbor, around 5 Å, as previously observed for 1,4-cis polybutadiene [21].

#### Glass Transition Temperature Predictions Using Molecular Dynamics Simulations

On the lowest energy model of each system, NPT simulations were performed at various temperatures to determine the average values of the volume and specific volume for the model.

Many factors can affect the reliability of the simulated model and therefore, of the predicted  $T_g$  values. It has been shown that simulation time does not affect significantly the final  $T_g$  value as determined by molecular dynamics [27]. Model quality is however of utmost importance. For instance, a model poorly equilibrated, or a very small model, yield no accurate  $T_g$  values. Therefore, in this work, care was taken to verify, before using the simulations for density evaluation, that internal, external, and density were fluctuating around a mean value. Fried and Ren have shown that thermal expansion values are very sensitive to unit cell dimensions, and a 15 K overestimation was observed for polysilanes in such a case [27]. Therefore, to ascertain if cell size was correct for the type of molecules modeled in the present case, two cell-sized models were built for HTPB and labeled Models one and two. As can be seen from Table 2,  $T_g$  determination using these two models varied from only one degree, well within the error that can be estimated from normal temperature fluctuations in molecular dynamics simulations. This, therefore, confirms that the cell size used is sufficient to insure reliable  $T_g$  estimations for these systems. As expected from statistical considerations, however, a larger model results in smaller data fluctuations, and therefore a smaller estimated uncertainty when determining  $T_g$  by the molecular dynamics approach. On the other hand, the price required, computer-time wise, for this

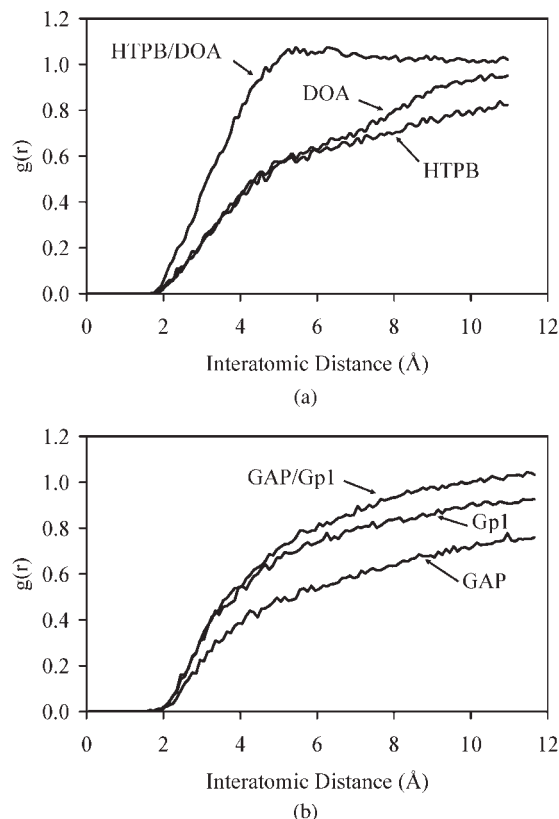


FIG. 4. Intermolecular pair correlation function  $g(r)$ ; (a) HTPB-DOA blend and (b) GAP/GPI blend.

additional precision is high, and it was therefore chosen in this work to perform calculations on the smaller systems.

Specific density values are plotted as a function of temperature in Fig. 5 for pure components and blends studied. As can be seen, an inflection point can clearly be detected, and linear regression was used to establish equations for two linear relationships. The first, observed at low temperatures, is related to the glassy state and is shown as a continuous straight line established with data drawn as full circles. The second, at higher temperatures, corresponds to the rubbery state, is drawn with a dotted straight line, and is calculated using data points drawn with open symbols. The correlation bands for each of these datasets appear on each side as finer full or dotted lines. In the case of Fig. 5a, the correlation band for the glassy state are so close to the straight line that it cannot be distinguished from it. In all cases, the correlation band is small for the glassy state, in keeping with the low data point dispersion and low fluctuations for this phase, uncertainty being mostly associated to the determination of the rubber phase, which shows higher data point dispersion, lower correlation coefficients, and larger correlation bands.

$T_g$  values calculated using this molecular modeling approach,  $T_{g, MD}$ , are reported in Table 2, along with

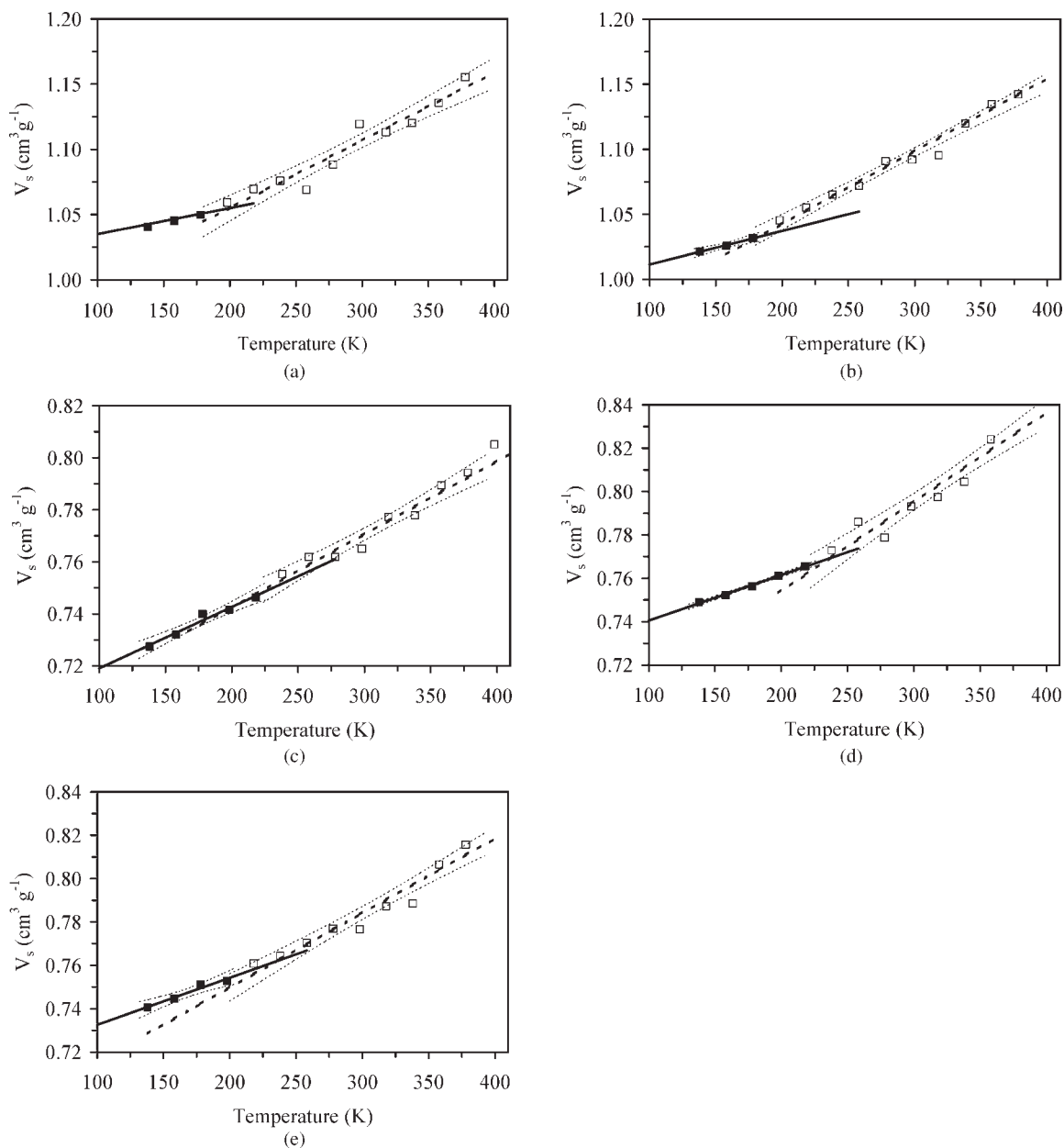


FIG. 5. Changes in specific volume during molecular dynamics simulations at various temperatures. (Lines represent linear regression results. Filled symbols correspond to data used for the regression shown as full lines, and open symbols to the one shown as dotted lines). (a) HTPB Model 1, (b) HTPB/DOA, (c) GAP, (d) GPI, and (e) GAP/GPI.

correlation coefficients for the two linear curves, as well as experimental and calculated values. For the low-temperature curve, pertaining to the glassy phase, few data were used, as it is well known that the behavior is highly linear in this temperature region. Correlation coefficients are therefore very high (0.96–1.00). Slightly lower values are obtained for the higher temperature curve, related to the rubbery phase (0.88–0.98). This is the main uncertainty source for  $T_g$  prediction by molecular dynamics, although intrinsic limitations due to the force field parameterization are always present. Other factors, limiting the appropriateness between modeled and real systems,

included structural differences between the two, which are often difficult to correct due to limited available information on structural defects, end groups, and impurities. Indeed, the difference experimental data from literature and measurement in this work varies from 3 to 10 K, due solely to variations in polymers and experimental conditions. When comparing MD results to experimental values, using the  $\Delta T_{g, \text{MD-exp}}$  value reported in Table 2, a 2–20 K variation is observed, MD systematically overestimating  $T_g$ . This is expected, as it has clearly been shown that the high cooling speed used during simulation when compared with experimental conditions ( $\sim 5^\circ/150$  ps, or



$3 \times 10^{-9}$  °/s for modeling versus 10°/min or 0.2°/s for DSC), result in overestimation of  $T_g$  due to kinetic effects [16]. Under these conditions, modeled systems do not reach equilibrium conditions, as long-range movements occurring at  $T_g$  do not have time to occur during the dynamics simulations. Lyulin et al. [33] as well as Soldéra and Métatla [34] have proposed to use the time-temperature superposition principle to correct for this overestimation, using respectively the Vogel-Fulcher-Tammans and the Williams-Landel-Ferry (WLF) equations. However, the overestimation observed here is much lower than that observed by Soldéra and Metatla, whereas it should be the same if the WLF equation applies to all polymers using universal parameters. Further work will be needed to ascertain whether the WLF equation is applicable for all modeled systems, including low molecular weight molecules such as those studied here.

Of more interest, in this case, is to compare the effect of plasticizer on with respect to  $T_g$  of the blends, as reported in Table 3 as the predicted  $\Delta T_g$  values from MD. In this respect, molecular dynamics fares much better, as the kinetic effect due to rapid cooling rates is the same for the modeled polymer and blend. The experimental  $\Delta T_g$  value of 14 K is not reproduced by any predictive method used here, but MD as well as Fox and Pochan equations give the same very good fit, with a 12 K prediction, only 2 K overestimated when compared with experimental data. More importantly, a very good fit is also observed for the HTPB/DOA system, with values of 15 K for experiments and 18 K for modeling. In this case, in the absence of data for pure DOA, no other predictive method was applicable.

## CONCLUSION

The glass transition temperature is a good measure of the degree of insensitivity a polymer blend will impart to a plastic-bonded explosive material. Although its experimental determination is the final, absolute decision criteria, methods to estimate  $T_g$  values before measurements are sought for a first screening. Molecular modeling, first proposed 20 years ago by Rigby and Roe, provides an efficient way to predict this property for pure polymers, small molecules, and blends. The present investigation on energetic systems has shown a very good agreement with experimental values, and comparable to those obtained using a much faster approach, using experimental values of pure polymer  $T_g$ s and the Fox equation.

The great difference in heating rates between modeling and experimental measurements, which can be several orders of magnitude, did not affect absolute  $T_g$  values by more than 20 K, molecular dynamics models always leading to overestimated values. A better fit was found regarding the effect of plasticizer on polymer  $T_g$ , using the difference in  $T_g$  between pure polymer and blend  $\Delta T_g$ , which was only different from experimental values by 2–3 K.

Because of its relatively high computer simulation times, it is proposed that molecular dynamics be used in priority for systems for which traditional approaches are not possible (such as in the absence of the  $T_g$  value of one or more pure component), when miscibility is not known or for screening purposes of plasticizers prior to their synthesis. This technique could also be worthwhile using when strong interactions are expected in a given polymer-plasticizer blend. Finally, although it can be used as a predictive method, it is far from the sole usefulness of molecular dynamics simulations of  $T_g$ . Its most spectacular contribution could lie in a better understanding of the processes occurring during glass transition, for which experimental techniques provide limited insight.

## ACKNOWLEDGMENTS

The authors acknowledge the support of the Centre de Bio-informatique et de Biologie Computationnelle of Laval University for its help with computer issues. The authors gratefully thank the scientists P. Lessard and P. Brousseau from DRDC Valcartier for the fruitful discussions they had with them on all experimental data of polymer and plasticizers used in this work.

## REFERENCES

1. R.G. Stacer and D.M. Husband, *Propellants, Explosives, Pyrotech.*, **16**, 167 (1991).
2. J.H. Gibbs and S.F. DiMarzio, *J. Chem. Phys.*, **28**, 373 (1958).
3. M. Doi and S.F. Edwards, *Theory of Polymer Dynamics*, Clarendon Press, Oxford (1986).
4. D. Rigby and R. J. Roe, *Macromolecules*, **23**, 5312 (1990).
5. L.H. Sperling, *Introduction to Physical Polymer Science*, Wiley-Interscience, New York (1986).
6. L.A. Wood, *J. Polym. Sci.*, **28**, 319 (1958).
7. T.G. Fox, *Bull. Am. Phys. Soc.*, **2**, 123 (1956).
8. J.M. Pochan, C.L. Beatty, and D.F. Pochan, *Polymer*, **20**, 879 (1979).
9. J.S. Gordon and M.J. Taylor, *J. Appl. Chem.*, **2**, 495 (1952).
10. A.J. Kovacs, *Polym. Sci.*, **3**, 394 (1961).
11. H.A. Schneider, *Polymer*, **30**, 771 (1990).
12. T.G. Kwei, *J. Polym. Sci. Polym. Lett. Ed.*, **22**, 307 (1984).
13. R. Simha, *Rheol. Acta.*, **14**, 12 (1975).
14. T. Somecynsky and R. Simha, *J. Appl. Phys.*, **42**, 4545 (1971).
15. D. Rigby and R.J. Roe, *J. Chem. Phys.*, **87**, 7285 (1987).
16. J. Han, R.H. Gee, and R.H. Boyd, *Macromolecules*, **27**, 7781 (1994).
17. L. Yang, D.F. Srolovitz, and A.F. Yee, *J. Chem. Phys.*, **110**, 7058 (1999).
18. J. Takeuchi and R.J. Roe, *J. Chem. Phys.*, **94**, 7458 (1991).
19. R.H. Boyd, *Trends Polym. Sci.*, **4**, 12 (1996).
20. J. Buchholz, W. Paul, and K. Binder, *J. Chem. Phys.*, **117**, 7364 (2002).

21. T.C. Clancy, M. Pütz, J.D. Weinhold, J.G. Curro, and W.L. Mattice, *Macromolecules*, **33**, 9452 (2000).
22. K.G. Wagner, M. Maus, A. Kornherr, and G. Zifferer, *Chem. Phys. Lett.*, **406**, 90 (2005).
23. Sartomer Application Bulletin, "Poly Bd<sup>®</sup> Resins With Low Hydroxyl Functionality," Sartomer Inc. (2005).
24. H. Sun, P. Ren, and J.R. Fried, *Comput. Theor. Polym. Sci.*, **8**, 229 (1998).
25. J.R. Fried and P. Ren, *Comput. Theor. Polym. Sci.*, **9**, 111 (1999).
26. M. Fukuda and H. Kikuchi, *J. Chem. Phys.*, **113**, 4433 (2000).
27. J.R. Fried and B. Li, *Comput. Theor. Polym. Sci.*, **11**, 273 (2001).
28. S. Bunte and H. Sun, *J. Phys. Chem. B*, **104**, 2477 (2000).
29. L.A. Utracki, *Polym. Technol.*, **5**, 33 (1985).
30. H.W. Kammer, J. Kressler, and C. Kummerloewe, *Polym. Sci.*, **106**, 31 (1993).
31. GAP Gumstock Results, JANNAF Propulsion Meeting, Indianapolis, 3M Corp. (1992)
32. H. Abou-Rachid, X. Lafleur-Lambert, L.S. Lussier, M. Jaidann, N. Gagnon, and J. Brisson, *Modélisation de l'effet de plastifiants sur la température de transition vitreuse du polybutadiène et du polyglycidylazide*, Technical Report, Defence Research and Development Canada-Valcartier, submitted, June (2007).
33. A. V. Lyulin, N. K. Balabaev, and MAJ. Michels, *Macromolecules*, **36**, 8574 (2003).
34. A. Soldera and N. Metatla, *Phys. Rev. E*, **74**, 061803 (2006).